The Internal Timescale of High Polymers*

BY

Shigeharu ONOGI

Department of Textile Chemistry

(Received December, 1954)

Synopsis

The dynamic viscosity η and the imaginary part of the complex dynamic compliance J'' of many high polymers measured in frequency ranges, which are remote from the region of the anomalous dispersion of the complex dynamic modulus, conform to the following equations, respecitively:

$$\frac{1}{\tau_2^2}\cdot\frac{1}{\omega^2}(\eta-\eta_2-\eta_3)+(\eta-\eta_3)=0,$$

and

$$\frac{1}{\tau_2^2}\cdot\frac{1}{\omega^2}\cdot\frac{\eta_2}{\eta_2+\eta_3}\left(\frac{1}{J''\omega}-\eta_3\right)+\left(\frac{1}{J''\omega}-\frac{\eta_2\eta_3}{\eta_2+\eta_3}\right)=0,$$

where, η_2, η_3 and τ_2 are constants, and ω is angular frequency. The first equation is the one used by Lyons, which is a modified form of the one used by Tobolsky and Eyring. Both the internal timescales, τ_2 in these equations, depend solely upon the experimental timescale and are independent of the nature of materials to be tested and of the environmental conditions. The values of τ_2 obtained from the data in the frequency range of the order of 10–10^2 cps are not of the order of second, as was erroneously reported by the previous authors, but of 10^{-3} second. The internal timescale of the order of seconds can only be obtained in much lower frequency range of 10^{-2}–10^{-1} cps. Thus, it seems very difficult to correlate the parameters of mechanical models simply with molecular mechanisms. Some characteristics of dynamic properties of high-polymeric materials are also discussed. Furthermore, in the appendix, the analysis of viscoelastic hysteresis loop obtainable from the Wakeham-type of apparatus is described.

Introduction

It has long been recognized that the representation of complex types of viscoelastic behavior manifested by high-polymeric materials requires the introduction of a multiplicity of internal timescales (relaxation time or retardation time). In order

* Presented in part at the fourth annual meeting of the Chemical Society of Japan, Tokyo City, April 6–9 and at the First Rheology Symposium of the Society, Tokyo City, November 10–11, 1951, and in conclusive form at the High-Polymer Symposium of the Kansai-Branch of the High-Polymer Society of Japan, Kyoto City, November 20–22, 1952.

to represent such materials, either the Maxwell or the Voigt model composed of a number of corresponding elements in parallel or in series is usually employed. When each model is subjected to a sinusoidal strain or stress, the dynamic properties would be given as follows:

$$\text{Maxwell model} \begin{cases} E' = \sum E_i \dfrac{\omega^2\tau_i^2}{1+\omega^2\tau_i^2}, & \text{(1a)} \\ \eta = \sum \eta_i \dfrac{1}{1+\omega^2\tau_i^2}, & \text{(1b)} \end{cases}$$

$$\text{Voigt model} \begin{cases} J' = \sum \dfrac{1}{E_i} \cdot \dfrac{1}{1+\omega^2\tau_i^2}, & \text{(2a)} \\ J'' = \sum \dfrac{1}{E_i} \cdot \dfrac{\omega\tau_i}{1+\omega^2\tau_i^2}, & \text{(1b)} \end{cases}$$

where E', η, J' and J'' are dynamic modulus, dynamic viscosity, the real and imaginary part of the complex dynamic compliance, respectively. And E_i, η_i and τ_i denote partial modulus, viscosity and internal timescale of i'th element, respectively. Each element has a different value of internal timescale and hence manifests a different behavior for a particular experiment.

In the case of the Maxwell model, for instance, the elements with much longer or shorter relaxation times than the timescale of experimental investigation show ideal elastic or pure viscous responses, whereas, the elements having relaxation times comparable with the experimental timescale exhibit viscoelastic characteristics. Consequently, the dynamic modulus is composed of contributions from ideally elastic and viscoelastic elements, while the dynamic viscosity is composed of those from viscoelastic and purely viscous ones. Thus, it is probable that the dynamic properties can well be represented by simpler types of mechanical models even when one considers infinite distribution of internal timescales. These simple models are of the Maxwell and the Voigt types. Both of these are composed of three units, the first and third of which degenerate, respectively, into a spring and a dashpot representing a number of elastic

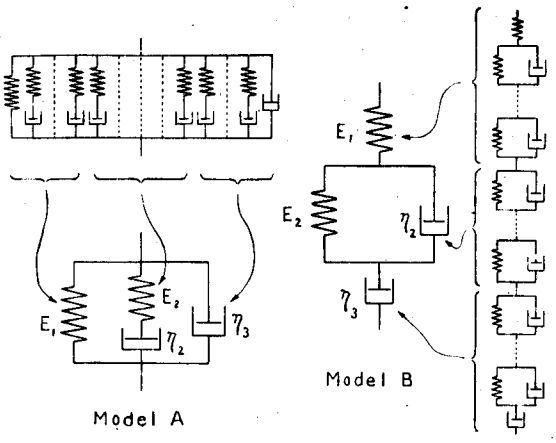

Fig. 1. Condensed mechanical models of the Maxwell and the Voigt types.

and viscous responses, while the second comprises a spring coupled with a dashpot representing a number of viscoelastic responses (Fig. 1 A and B). For such a Maxwell model, the dynamic modulus E' and viscosity η are given by the following equations:

$$E' = E_1 + E_2 \frac{\omega^2\tau_2^2}{1+\omega^2\tau_2^2}, \tag{3a}$$

and

$$\eta = \frac{\eta_2}{1+\omega^2\tau_2^2} + \eta_3 . \tag{3b}$$

The latter can be transformed into the following form in $1/\omega^2$ and η:

$$\frac{1}{\tau_2^2} \cdot \frac{1}{\omega^2}(\eta - \eta_2 - \eta_3) + (\eta - \eta_3) = 0 . \tag{4}$$

Eq. (3b) was discussed by Tobolsky and Eyring[1] while Eq. (4) was used by Lyons[2] to analyze dynamic-property data obtained in the frequency range of the order of 10–10^2 cps. According to these authors, τ_2 is the relaxation time corresponding to the secondary-bond processes. Tobolsky and Eyring postulated that τ_2 is of the order of seconds. It has been found, however, as will be shown below, that τ_2 has a certain average relaxation time of a number of mechanisms which manifest viscoelastic responses. Thus, the value of τ_2 depends merely on the timescale of a particular experiment and is independent of the nature of materials to be tested and of the environmental conditions such as temperature and humidity. The values of τ_2 obtainable from data in the frequency range of the order of 10–10^2 cps are not of the order of seconds[2] but of 10^{-3} second, and it seems very difficult to correlate the parameters of mechanical models simply with molecular mechanisms.

The present paper is to verify this new concept of relaxation time by analyzing dynamic-property data of many different solid high polymers obtained from experiments of long and short timescales. Some common characteristics of dynamic properties of high-polymeric materials are also described.

Short Timescale Experiments

In the previous paper[3], dynamic moduli of elasticity and dynamic viscosities of several high polymers such as viscose monofils, polycaprolactam film and polyvinyl chloride films were measured in a frequency range of 20–200 cps at around 20–25°C

1) A. Tobolsky, and H. Eyring, J. Chem. Phys., **11**, 125–34 (1943).
2) W. J. Lyons, J. Appl. Phys., **21**, 520–2 (1950). In private communication with Dr. W. J. Lyons it was agreed on that the value for τ_2 in his article should have been $2.94 \cdot 10^{-3}$ second instead of 9.3 seconds.
3) M. Horio, S. Onogi, C. Nakayama, and K. Yamamoto, J. Appl. Phys., **22**, 966–70 (1951).

except as noted in Table I and II by employing the vibrating reed method[4], and viscoelastic properties of these materials were discussed from various points of view. Using these data, the dynamic viscosities have been analyzed by means of the graphic method of Lyons to obtain the values of the constants η_2, η_3 and τ_2 in Eq. (4). It has been found that, in all the cases studied, the η vs. $1/\omega^2$ plot and the η vs. $1/\omega$ plot could well be represented by a hyperbola and a cubic, respectively, as required by Eq. (4); and, in particular, the latter was practically represented by a straight line as pointed out by Lyons[5]. Several examples are reproduced in Figs. 2–5. The results of calculations are listed in Table I, together with those of Lyons (See the column "Model A").

A fact worth noting is that the values of τ_2 for all these specimens are not of the order of seconds but of 10^{-3} second, and are almost equal for all specimens noticeably differing in their nature, though they are apt to become smaller with the elevation of the frequency range of the experiments. Furthermore, it is seen from the table that the values of τ_2 are also independent of the temperatures at which the dynamic measurements were performed, as is shown in the case of vulcanized rubber, though the other characteristics such as η_2 and η_3 vary remarkably with temperature.

The values under the heading "$\omega_m\tau_2$" are the products of τ_2 and the arithmetical mean of angular frequencies at both the limits of the experimental range, ω_m. They might be regarded as almost constant in all cases if one makes allowances for the precision of the experiments and for great differences in the values of ω_m.

Now, in the case of Model B in Fig. 1, we have the following equation similar to Eq. (4):

$$\frac{1}{\tau_2^2}\cdot\frac{1}{\omega^2}\cdot\frac{\eta_2}{\eta_2+\eta_3}\left(\frac{1}{J''\omega}-\eta_3\right)+\left(\frac{1}{J''\omega}-\frac{\eta_2\eta_3}{\eta_2+\eta_3}\right)=0\,, \qquad (5)$$

where, η_2, η_3 and τ_2 are constants. This equation will represent experimental results as satisfactorily as Eq. (4) did for Model A. The above three constants evaluated by means of the same graphical method are summarized in Table I (See the column "Model B"). The values of τ_2 thus obtained are also of the order of 10^{-3} second and have almost the same special features as in the previous case. Although the claim of constancy for the values of products $\omega_m\tau_2$ is not so valid as before, the differences in these values are exceedingly small as compared with those of the values of ω_m.

In the treatments of the foregoing authors (Model A), $\omega\tau_3$ was neglected after considering that it was much smaller than unity, while in the case of Model B just

4) M. Horio, and S. Onogi, J. Appl. Phys., **22**, 977-81 (1951).
5) W. J. Lyons, loc. cit.

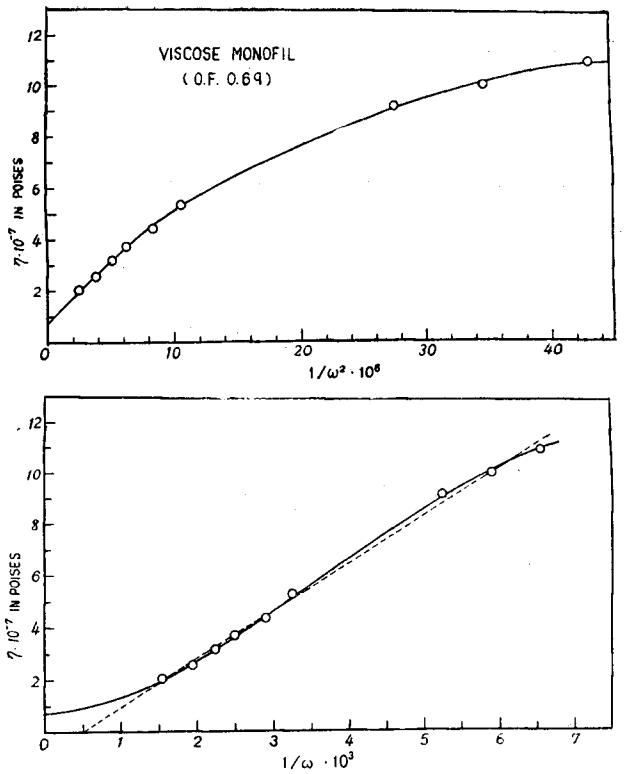

Fig. 2. η vs. $1/\omega^2$ and $1/\omega$ for viscose monofil.

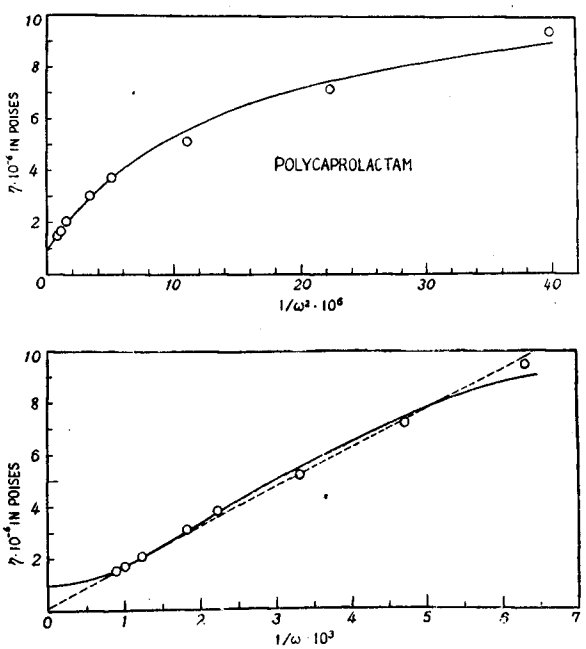

Fig. 3. η vs. $1/\omega^2$ and $1/\omega$ for polycaprolactam film.

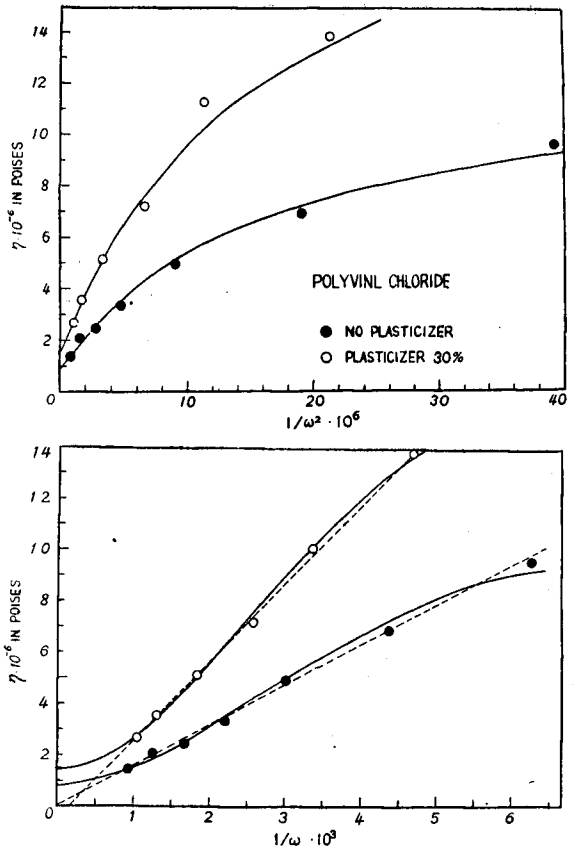

Fig. 4. η vs. $1/\omega^2$ and $1/\omega$ for polyvinyl chloride films.

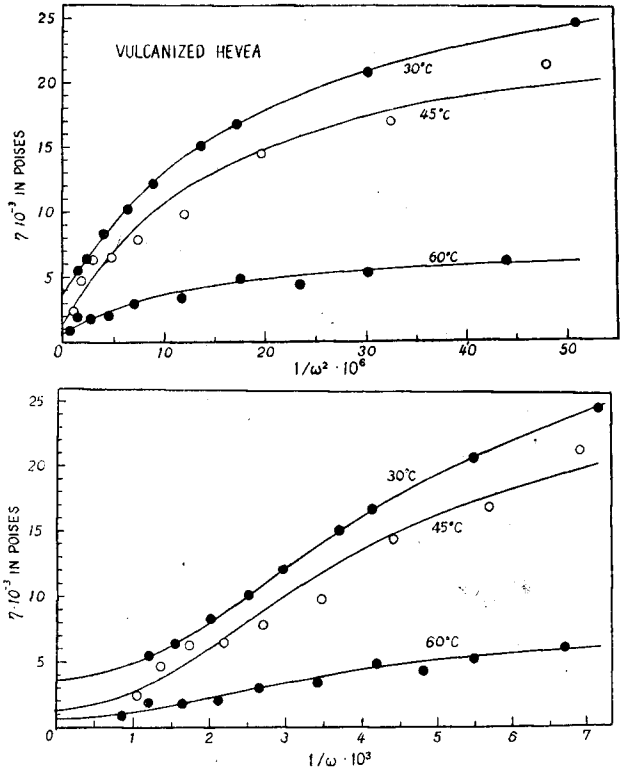

Fig. 5. η vs. $1/\omega^2$ and $1/\omega$ for vulcanized Hevea sheet.

Table I. Parameters for Model A and B.

Specimen	Frequency range, cps	Average angular frequency, ω_m	MODEL A				MODEL B			
			η_2, poises	η_3, poises	τ_2, second	$\omega_m\tau_2$	η_2, poises	η_3, poises	τ_2, second	$\omega_m\tau_2$
			SHORT TIMESCALE EXPERIMENTS							
Viscose monofil (O.F. 0.69)	24.2–102	397	$18.3\cdot10^7$	$0.736\cdot10^7$	$5.71\cdot10^{-3}$	2.26	$4.33\cdot10^9$	$9.67\cdot10^9$	$1.72\cdot10^{-3}$	0.684
Cellulose acetate film	23.2–161	579	$15.0\cdot10^6$	$0.881.10^6$	4.76· ″	2.76	$0.345\cdot10^9$	3.89· ″	0.892· ″	0.516
Polycaprolactam film	25.2–178	638	$11.1\cdot10^6$	$0.993.10^6$	3.97· ″	2.53	$0.434\cdot10^9$	3.46· ″	0.776· ″	0.495
Polyvinyl chloride film (no plasticizer)	25.4–172	620	$11.9\cdot10^6$	$0.803\cdot10^6$	4.02· ″	2.49	$0.601\cdot10^9$	4.78· ″	0.971. ″	0.577
Polyvinyl chloride film (plasticizer 30%)	34.0–155	594	$21.2\cdot10^6$	$1.43\cdot10^6$	4.00· ″	2.38	$1.23\cdot10^8$	$6.34\cdot10^8$	1.24· ″	0.735
Vulcanized Hevea										
30°C	22.5–132	486	$30.7\cdot10^3$	$3.64\cdot10^3$	4.80· ″	2.33	$0.616\cdot10^5$	$20.2\cdot10^5$	1.52· ″	0.737
45°C	23.0–151	547	25.2· ″	1.25· ″	4.06· ″	2.22	$1.27\cdot10^5$	18.4· ″	1.58· ″	0.862
60°C	24.0–188	666	6.83· ″	0.610·″	3.52· ″.	2.34	$1.20\cdot10^5$	14.8· ″	1.26· ″	0.842
Nylon monofil (By Lyons)	about 50–300	1100	$12.4\cdot10^6$	$1.13\cdot10^6$	$2.94\cdot10^{-3}$*	3.23				
Butyl rubber	30–500	1665	$20.5\cdot10^3$	$3.11\cdot10^3$	$1.94\cdot10^{-3}$	3.22	$2.58\cdot10^5$	$50.0\cdot10^5$	$0.842\cdot10^{-3}$	1.37
(By Ivey, Mrowca, Guth)	$3\cdot10^5$–$5\cdot10^6$	$1.665\cdot10^7$	359	63.2	$1.65\cdot10^{-7}$	2.75	$4.24\cdot10^2$	$10.2\cdot10^2$	$5.11\cdot10^{-8}$	0.850
			LONG TIMESCALE EXPERIMENTS							
Vulcanized Hevea string	3.52–$15.9\cdot10^{-2}$	0.612	$16.6\cdot10^6$	$1.41\cdot10^6$	3.72	2.28	$1.26\cdot10^7$	$9.86\cdot10^7$	1.16	0.707
Plasticized polyvinyl chloride film	3.91–$38.3\cdot10^{-2}$	1.32	$12.9\cdot10^7$	$0.622\cdot10^7$	2.21	2.93	$3.38\cdot10^7$	$25.4\cdot10^7$	0.758	1.00

* The value reported by Lyons was 9.3 seconds.

mentioned it was assumed to be very much greater than unity and was also eliminated. In all these cases, equations which can be derived from Eqs. (1b) and (2b) without eliminating both τ_2 and τ_3, and which include consequently four constants η_2, η_3, τ_2 and τ_3, are not satisfied by the experimental results. In other words, no reasonable set of the above four constants as will satisfy the experimental results can be obtained by the graphical method.

Considering all these results, it follows that the dynamic viscosity or imaginary part of complex dynamic compliance multiplied with ω, measured in a rather narrow frequency range, can well be represented by a general equation

$$A(\xi-B)+\omega^2(\xi-C)=0, \tag{6}$$

or

$$\xi=C+\frac{A(B-C)}{A+\omega^2}, \tag{7}$$

where ξ denotes the dynamic viscosity η or the reciprocal of imaginary part of complex dynamic compliance multiplied by ω, $1/J''\omega$. This will mean that ξ is composed of two terms, one of which is dependent and the other is not dependent upon frequency. Three constants A, B and C in these equations represent the following quantities, respectively:

	Model A	Model B
ξ	η	$1/J''\omega$
A	$1/\tau_2^2$	$\eta_2/\tau_2^2(\eta_2+\eta_3)$
B	$\eta_2+\eta_3$	η_3
C	η_3	$\eta_2\eta_3/(\eta_2+\eta_3)$

As mentioned above, the fact that the products $\omega_m\tau_2$ are almost constant for all specimens having quite different properties, and are also independent of the environmental conditions, such as temperature, enables us to expect much shorter internal timescales from experimental data in higher frequency ranges.

For example, the dynamic-property data on butyl rubber studied by Ivey, Mrowca and Guth[6] in a higher frequency range was analyzed in quite the same manner as before, and the results compared. Although the dynamic viscosities in a frequency range in which an anomalous dispersion of complex dynamic modulus (elastic dispersion) occurs, decrease gradually with frequency and do not obey Eq. (7), those determined in the frequency ranges of 30–500 cps and $3\text{–}50\cdot10^5$ cps can well be treated as before. The results of calculation were also tabulated in Table I. As was expected, the higher the frequency range, the smaller the values of τ_2. But the products $\omega_m\tau_2$ had almost the same values as in the former cases.

6) D. G. Ivey, B. A. Mrowca, and E. Guth, J. Appl. Phys. **20**, 486-92 (1949).

Long Timescale Experiments

In the case of short timescale experiments described above, the internal timescale of the order of seconds was never encountered. If the constancy of the products $\omega_m\tau_2$ is always established regardless of the magnitude of timescales of the experimental investigations, internal timescales of the order of seconds might be expected when the dynamic measurements were carried out over a frequency range of about 10^{-1}–10^{-2} cps. It is rather difficult, however, to obtain frequency dependence of dynamic viscosities in such a lower frequency range because of the lack of a suitable apparatus. To effect these purposes, a new apparatus was constructed, and long timescale experiments were performed.

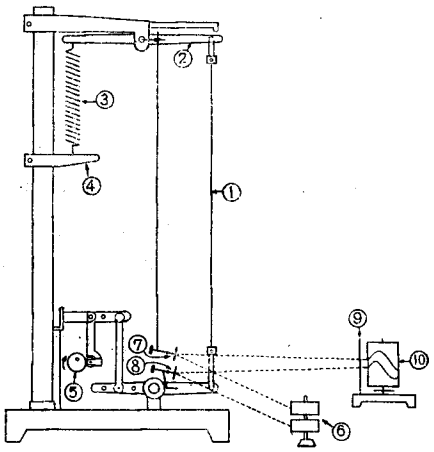

Fig. 6. Schematic diagram of the apparatus.

A schematic diagram of the apparatus is shown in Fig. 6. The sample (1) is suspended from one end of the rotatable lever (2) and counterbalanced with a calibrated spring (3) of suitable stiffness, which is extended from the other end of the lever to the adjustable arm (4). The lower end of the sample is subjected to a cyclic displacement of a given amplitude by means of a transmission assembly consisting of a variable speed motor, a set of speed reduction gears (not shown in the figure), an eccentric cam (5), and so on. The movements of both the ends of the sample are magnified to desirable extent and are recorded by the recording system. Thus, light beams from the sources (6) are reflected by two mirrors (7, 8), which can move up and down in response to the movements of both the ends of the sample, and after being condensed by a cylindrical lens (9) to spots, they are projected on a photographic paper mounted on the rotating drum (10). The frequency and amplitude of the mirrors could be varied over rather wide ranges.

By means of this apparatus, the two traces of the displacements of the two ends of the sample can be obtained as a function of time on the photographic paper. They have some phase difference from each other, which arises from a damping (or viscous) effect of the sample. The extension of the sample may be obtained from the difference between these two traces divided by the magnifications, and the upper trace on the photograghic paper gives the elongation of the spring, which can be converted to the stress in the sample as a function of time from the load-elongation relationship of the spring. By analyzing these two waves of the extension and the

stress, it is possible to determine the dynamic modulus of elasticity (Young's modulus) as well as mechanical loss factor, and hence, dynamic viscosity of the sample. (See Appendix.)

Typical dynamic-viscosity data were treated in quite the same manner as in the short timescale experiments. The results of calculation are also included in Table I. As was expected, the internal timescales of the order of seconds were obtained in these studies, but there is not much change in the values of the products $\omega_m\tau_2$ as compared with those obtained previously.

Discussion

The dynamic viscosity measured within the frequency range widely differing from that of the anomalous dispersion decreases rapidly with increasing frequency in such a manner that the product of the viscosity and the frequency is approximately constant, while in the region of the anomalous dispersion of the complex dynamic modulus (elastic dispersion) it decreases more slowly with increasing frequency. The viscosity of the first type may be adequately expressed by Eq. (7) finding suitable values for the parameters η_2, η_3 and τ_2. The equation cannot be applied to the viscosity of the second type.

The fact that the plots of the dynamic viscosity against $1/\omega$ is practically linear reminds us of the box type distribution of relaxation (or retardation) times covering a considerably wide range, as described by Kuhn et al.[7] and Tobolsky et al.[8] In case the frequency range of experiments is much narrower compared with this distribution range and is entirely involved in it, the viscosity becomes directly proportional to $1/\omega$:

$$\eta = \frac{\pi}{2} \cdot \frac{G_0}{\omega}, \tag{4'}$$

where G_0 is constant. In the region of the anomalous dispersion, however, the box type distribution is no more available. Therefore, the relation expressed by Ex. (7) is clearly related to the simple (box) type distribution of internal timescales.

The constancy of the product $\omega_m\tau_2$ can be verified from the fact that $\hat{\xi}$ vs. $1/\omega$ curve can be approximately replaced by a straight line passing through the origin*. For the cubic curve which conforms to Eq. (7) the angular frequency ω and $\hat{\xi}$ at the point of inflection can be obtained by setting the second derivative of $\hat{\xi}$ with respect to $1/\omega$ equal to zero:

$$\omega_i = (3A)^{\frac{1}{2}}, \tag{8a}$$

7) W. Kuhn, O. Künzle, and A. Preissmann, Helv. Chim. Acta, **30**, 307, 464, 839 (1947).
8) A. V. Tobolsky, B. A. Dunnel, and R. D. Andrews, Textile Research J., **21**, 404 (1951).
* The author is much indebted to Dr. H. Fujita for his helpful discussion and suggestion.

and

$$\hat{\xi}_i = \frac{1}{4}(B+3C)\,. \tag{8b}$$

When the tangent at this point passes through the origin, the following relation can be obtained between the values of the asymptote, B, and the intercept, C:

$$B = 9C\,. \tag{9}$$

If the experimental values range from C to B on this tangent, $\hat{\xi}$, B and C would be given by the equations—

$$\hat{\xi} = \frac{3}{8}(B-C)\omega_i/\omega\,, \tag{7'}$$

$$B = \frac{3}{8}(B-C)\omega_i/\omega_1\,, \tag{10a}$$

and

$$C = \frac{3}{8}(B-C)\omega_i/\omega_2\,. \tag{10a}$$

Then, we obtain

$$\omega_1 = \omega_i/3\,, \tag{11a}$$

and

$$\omega_2 = 3\omega_i\,. \tag{11b}$$

Hence, the arithmetical and geometrical means, ω_{ma} and ω_{mg}, of ω_1 and ω_2 are, respectively, given as follows:

$$\omega_{ma} = \frac{5}{3}\omega_i = \frac{5}{3}(3A)^{\frac{1}{2}}, \tag{12a}$$

and

$$\omega_{mg} = \omega_i = (3A)^{\frac{1}{2}}. \tag{12b}$$

For Model A, therefore, we obtain

$$\omega_{ma}\tau_2 = 2.89\,,$$

$$\omega_{mg}\tau_2 = 1.73\,,$$

since A denotes $1/\tau_2^2$ (See p. 50). And for Model B, we obtain

$$\omega_{ma}\tau_2 = 0.962\,,$$

$$\omega_{mg}\tau_2 = 0.577\,,$$

since A denotes $\eta_2/\tau_2^2(\eta_2+\eta_3)$, which is equal to $C/B\tau_2^2$ or $1/9\tau_2^2$ (See p. 50 and Eq. (7)).

Because the arithmetical and geometrical means of the angular frequencies in our experiments are not necessarily in accordance with ω_{ma} and ω_{mg} and the tangent at the point of inflection of the cubic does not always pass through the origin, the

values of $\omega_m\tau_2$ in Table I and those of $\omega_m'\tau_2$ (ω_m' denotes geometrical mean of angular frequencies at both the limits of the experimental range) in Table II differ more or less from the values of $\omega_{ma}\tau_2$ and $\omega_{mg}\tau_2$ which were deduced above. But the differences are not so great.

Table II. The constancy of the product $\omega_m'\tau_2$ for Model A and B.

Specimen	Geometrical mean of angular frequencies, ω_m',	$\omega_m'\tau_2$	
		Model A	Model B
	SHORT TIMESCALE EXPERIMENTS		
Viscose monofil (O.F. 0.69)	312	1.78	0.537
Cellulose acetate film	384	1.83	0.343
Polycaprolactam film	421	1.67	0.327
Polyvinyl chloride film (no plasticizer)	415	1.67	0.403
Polyvinyl chloride film (plasticizer 30%)	456	1.82	0.565
Vulcanized Hevea			
30°C	342	1.64	0.520
45°C	370	1.50	0.585
60°C	422	1.49	0.532
Nylon monofil (By Lyons)	770	2.06	
Butyl rubber (By Ivey,	770	1.49	0.634
Mrowca, Guth)	$7.70\cdot10^6$	1.27	0.393
	LONG TIMESCALE EXPERIMENTS		
Vulcanized Hevea string	0.470	1.75	0.545
Plasticized polyvinyl chloride film	0.769	1.70	0.583

As was often emphasized, one cannot obtain τ_2 of the order of seconds from the data obtained in the frequency range of the order of 10–10^2 cps, as was erroneously pointed out by the previous authors, but from those measured in much lower range of 10^{-2}–10^{-1} cps. Therefore, if the true values of the relaxation time for secondary-bond processes were the order of seconds, the relaxation times obtained in our long timescale experiments might, indeed, correspond to this type of relaxation mechanism, while the relaxation times of much smaller values obtained by us in the short timescale experiments could not be assumed to be of such a type of relaxation, but to correspond to another type of relaxation mechanisms. But it is rather difficult to differentiate the responding molecular mechanisms only by such a difference in their internal timescales. Thus, it is very questionable to correlate the parameters of mechanical models simply with various molecular mechanisms.

At any rate, it seems reasonable to consider that there exist in high polymers a number of mechanisms with different internal timescales. When such a material is subjected to a sinusoidal stress or strain of a particular angular frequency, both

the dynamic modulus and the viscosity are composed of the contributions from mechanisms having internal timescales comparable with the reciprocal of angular frequency, and from those having internal timescales far different from the reciprocal of the angular frequency. The first component is, therefore, dependent and the second is not dependent upon the frequency. As the frequency is increased, the dynamic viscosity will become lower and lower, since the mechanisms which have greater internal timescales must lose their contributions to the dynamic viscosity. With this change in frequency, of course, the dynamic modulus is also changed. Thus, the viscoelasticity of high polymers are always dependent upon the timescale of experimental investigation.

Eq. (7) is also applicable to the dynamic viscosity of solutions of polyvinyl alcohol measured by the electromagnetic transducer method over a frequency range from 45 to 300 cps. Here again, the calculated values of τ_2 are also of the order of 10^{-3} second, and the products $\omega_m\tau_2$ are almost constant and equal to those of solid high polymers. They are also independent either of the degree of polymerization of the solute polymers or of temperatures at which the measurements were carried out. Details will be published later[9].

Acknowledgment

The author wishes to express his sincere gratitude to Professor M. Horio for his kind guidance and encouragement to his studies. He also wishes to express acknowledgment to Professor Y. Sawaragi of the Department of Applied Physics and Assistant Professor H. Fujita of the Department of Fisheries, Kyoto University, for their helpful discussion, and also to Dr. W. J. Lyons of the Firestone Tire and Rubber Company for his useful comments.

APPENDIX

Analysis of Viscoelastic Hysteresis Loop

In the dynamic measurements of high-polymeric materials such as rubberlike and textile materials, the determination of viscoelastic hysteresis loop as a measure of consumption of mechanical energy, as heat, is often employed. This method is very useful, particularly in the lower frequency ranges. Energy loss, for instance, of various types of tire cords and constituent fibers have been extensively studied by Wakeham and his co-workers[10-12] by measuring hysteresis loops. Breazeale and

9) S. Onogi, and H. Hirai, unpublished work.
10) H. Wakeham, E. Honold, and E. L. Skau, J. Appl. Phys., **16**, 388-401 (1945).
11) H. Wakeham, and E. Honold, J. Appl. Phys., **17**, 698-711 (1946).
12) H. Wakeham, and E. Honold, Textile Res. J., **21**, 1-5 (1951).

Whisnant[13] have also measured energy losses in tire cords in quite the same manner.

In such measurements, it is often desired to relate the loop to other viscoelastic characteristics, such as dynamic modulus of elasticity, dynamic viscosity, mechanical loss tangent and so on, in order to compare the results with those obtained by means of other experimental methods, which give directly these characteristics.

The present article is concerned with the analysis of the viscoelastic hysteresis loop obtained by the Wakeham-type of apparatus.

In the apparatus used by Wakeham[12] in his studies on fibers, a test sample is fixed at its one end and is subjected to an external sinusoidal deformation of a given frequency and amplitude through a calibrated spring, which is connected in series with the sample. The extension of the spring can be converted to stress. Although the junction moves also sinusoidally with the same frequency, it manifests phase lag because of damping (or viscous) effect of the sample. Therefore, plotting both the movements of two ends of the spring on coordinate paper, a hysteresis loop can be obtained, whose area gives directly the energy loss of the sample.

Now, considering conventionally that the sample is analogous to the so-called Voigt element composed of a spring coupled in parallel with a dashpot, the system can well be represented by a mechanical model shown in Fig. 8. The fundamental

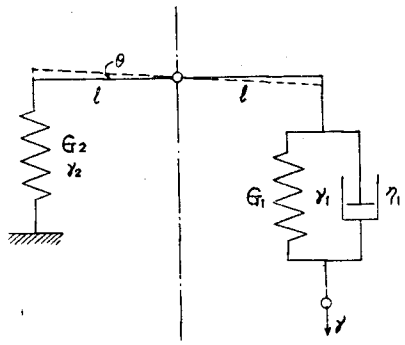

Fig. 7. Mechanical model for the apparatus with sample.

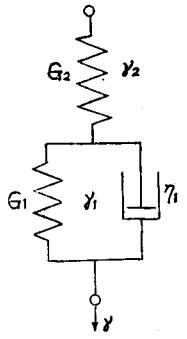

Fig. 8. Simpler model for the apparatus with sample.

equation of this model is given by Eq. (18) which is given later.

An apparatus constructed by us is similar in its principle to that of Wakeham. Its schematic diagram is shown in Fig. 6. Considering conventionally again that the sample can be substituted with a Voigt element, our apparatus is represented by a mechanical model shown in Fig. 7. The notation of various quantities involved are summarized as follows:

13) F. Breazeale, and J. Whisnant, J. Appl. Phys., **20**, 621-6 (1949).

S: tension in the sample and the spring, dynes
γ_1: extension of the sample, cm
G_1: spring (force) constant of the sample, dynes/cm
η_1: viscous force constant of the sample, dynes·sec/cm
L: length of the sample, cm
A: cross-sectional area of the sample, cm^2
$q=L/A$: shape factor of the sample, cm^{-1}
$E=qG_1$: Young's modulus of the sample, dynes/cm^2
$\eta=q\eta_1$: viscosity coefficient of the sample, dynes·sec/cm^2
l: length of arm of the lever, cm
θ: angle of rotation of the lever, radian
I: moment of inertia of the lever, g·cm^2
γ: external displacement, cm
G_2: spring constant of the calibrated spring, dynes/cm
γ_2: extension of the spring, cm

Then, the fundamental equation of motion of the system is given by the equation:

$$I\frac{d^2\theta}{dt^2}+G_2\theta l^2-G_1 l(\gamma-\theta l)-\eta_1 l\left(\frac{d\gamma}{dt}-l\frac{d\theta}{dt}\right)=0. \tag{17}$$

When the product of the moment of inertia of the lever and the square of angular frequency, $I\omega^2$, is negligible as compared with G_2l^2, as it was in our case, the inertia term in the left-hand side of the above equation can be safely neglected. Moreover, such being the case, the angle of rotation of the lever is very small, θl is equal to the extension of the spring, γ_2. Thus, the above model reduces to the simple one already shown in Fig. 8, and the fundamental equation of this model would be—

$$\left(G_1+\eta_1\frac{d}{dt}\right)\gamma=\left(\frac{G_1+G_2}{G_2}+\frac{\eta_1}{G_2}\frac{d}{dt}\right)S. \tag{18}$$

Since the external deformation is given as $\gamma=\gamma_0e^{i\omega t}$, Eq. (18) can be rewritten as

$$\frac{dS}{dt}+\frac{G_1+G_2}{\eta_1}S=\frac{G_2}{\eta_1}(G_1+i\omega\eta_1)\gamma_0e^{i\omega t}. \tag{18'}$$

Hence, in the stationary state, S and γ_2 are, respectively, given as follows:

$$S=\gamma_0(A+iB)e^{i\omega t}=\gamma_0(A^2+B^2)^{\frac{1}{2}}e^{i(\omega t+\delta_1)}, \tag{19}$$

where,

$$A=G_2[G_1(G_1+G_2)+\omega^2\eta_1^2]/[(G_1+G_2)^2+\omega^2\eta_1^2], \tag{20}$$

$$B=\omega\eta_1G_2^2/[(G_1+G_2)^2+\omega^2\eta_1^2], \tag{21}$$

$$\tan\delta_1=B/A=\omega\eta_1G_2/[G_1(G_1+G_2)+\omega^2\eta_1^2], \tag{22}$$

and

$$\gamma_2 = S/G_2 = \frac{G_1(G_1+G_2)+\omega^2\eta_1^2+i\omega\eta_1 G_2}{(G_1+G_2)^2+\omega^2\eta_1^2}\gamma_0 e^{i\omega t}. \tag{23}$$

Therefore, the extension of the sample, γ_1, is given by the equation

$$\gamma_1 = \gamma - \gamma_2 = \gamma_0(C-iD)e^{i\omega t} = \gamma_0(C^2+D^2)^{\frac{1}{2}}e^{i(\omega t-\delta_2)}, \tag{24}$$

where,

$$C = G_2(G_1+G_2)/[(G_1+G_2)^2+\omega^2\eta_1^2], \tag{25}$$

$$D = \omega\eta_1 G_2/[(G_1+G_2)^2+\omega^2\eta_1^2], \tag{26}$$

$$\tan\delta_2 = D/C = \omega\eta_1/(G_1+G_2). \tag{27}$$

Now, shifting the origin of time by δ_2, we obtain

$$S = \gamma_0(A^2+B^2)^{\frac{1}{2}}e^{i\omega t}, \tag{10'}$$

and

$$\gamma_1 = \gamma_0(C^2+D^2)^{\frac{1}{2}}e^{i(\omega t-\delta)}, \tag{24'}$$

where,

$$\delta = \delta_1+\delta_2, \tag{28}$$

and hence,

$$\tan\delta = (BC+AD)/(AC-BD) = \omega\eta_1/G_1. \tag{29}$$

It is easily shown that the hysteresis loop which can be obtained by plotting the imaginary part of S against that of γ_1 is an ellipse having its center at the origin. The equation of this ellipse is given as follows:

$$a'\gamma_1^2+b'S^2 = \gamma_0^2(C^2+D^2)\sin^2\delta, \tag{30}$$

where,

$$a' = \frac{1}{2}\left\{1+m^2-\sqrt{(1-m^2)^2+4m^2\cos^2\delta}\right\},$$

$$b' = \frac{1}{2}\left\{1+m^2+\sqrt{(1-m^2)^2+4m^2\cos^2\delta}\right\},$$

and

$$m = (C^2+D^2)^{\frac{1}{2}}/(A^2+B^2)^{\frac{1}{2}}. \tag{31}$$

The area of the loop, therefore, is given by the equation

$$W = \pi\gamma_0^2\omega\eta_1\cdot(C^2+D^2) = \pi\omega\eta_1\cdot(\text{amplitude of strain of the sample})^2$$

$$= \pi\gamma_0^2 G_2^2\omega\eta_1/[(G_1+G_2)^2+\omega^2\eta_1^2]. \tag{32}$$

Since the amplitude of strain of the sample and the area of the loop can be determined experimentally, the viscous force constant, η_1, or the mechanical loss factor, $\omega\eta_1$, of the sample can be evaluated by this equation.

The spring constant of the sample, G_1, on the other hand, is given by the following equation, using the notations A, B, C and D:

$$G_1^2 = (A^2+B^2)/(C^2+D^2) - \omega^2\eta_1^2, \tag{33}$$

and hence,

$$G_1 \cong \frac{(\text{amplitude of the stress})}{(\text{amplitude of the strain})}\left[1 - \frac{1}{2}\omega^2\eta_1^2\frac{(\text{amplitude of the strain})^2}{(\text{amplitude of the stress})^2}\right]. \tag{34}$$

Now, plotting S against γ instead of γ_1, we obtain another loop different in its shape from that mentioned above. The equation of this loop can easily be obtained as follows:

$$a''\gamma^2 + b''S^2 = \gamma_0^2 \sin^2\delta_1, \tag{35}$$

where,

$$a'' = \frac{1}{2}\left\{1+m'^2-\sqrt{(1-m'^2)^2+4m'^2\cos^2\delta_1}\right\},$$

$$b'' = \frac{1}{2}\left\{1+m'^2+\sqrt{(1-m'^2)^2+4m'^2\cos^2\delta_1}\right\},$$

and

$$m' = (A^2+B^2)^{-\frac{1}{2}}.$$

This shows that the loop is also ellipse having its center at the origin, and the area W' of this ellipse is given by the following equation:

$$\begin{aligned} W' &= \pi\gamma_0^2 B = \pi\cdot(\text{amplitude of the external deformation}) \\ &\quad \times(\text{amplitude of the imaginary part of the stress}) \\ &= \pi\gamma_0^2\omega\eta_1 G_2^2/[(G_1+G_2)^2+\omega^2\eta_1^2]. \end{aligned} \tag{36}$$

Comparing Eq. (36) with Eq. (32), it is seen at once that the areas of the two ellipses are quite equal.

Then the dynamic viscosity "η", the dynamic modulus "E" and the mechanical loss tangent "$\tan\delta$" of the sample are respectively given by the following equations:

$$\eta = q\eta_1 = q\frac{W(=W')}{\pi\omega\cdot(\text{amplitude of the strain})^2}, \tag{37}$$

$$E = qG_1 \cong q\frac{(\text{amplitude of the stress})}{(\text{amplitude of the strain})} \times\left[1 - \frac{1}{2}\omega^2\eta_1^2\frac{(\text{amplitude of the strain})^2}{(\text{amplitude of the stress})^2}\right], \tag{38}$$

and

$$\tan\delta = \omega\eta/E. \tag{39}$$